Photovoltaic System Fault Identification Methodology based on I-V Characteristics Analysis

Salima Sarikh[1,2, a)] and Mustapha Raoufi[1] and Amin Bennouna[1] and Ahmed Benlarabi[2] and Badr Ikken[2]

[1] *Laboratory of Nanomaterials for Energy and the Environment, Faculty of Sciences Semlalia, Cadi Ayyad University Marrakesh, Morocco*
[2] *Green Energy Park Research Platform, (IRESEN) Souissi - Rabat, Morocco*
[a)] Corresponding author: sarikh.salima@gmail.com

Abstract. In the photovoltaic field, regarding the importance of sustainability, monitoring systems are a paramount component for yield assessment. Yet in the industrial production, fault detection remains a manually handled issue. However, faults are responsible for significant power loss and sometimes, even dramatically damages such as fire hazard or material deterioration. This paper presents a methodology for fault detection in the photovoltaic systems regarding the different impacts of faults on the I-V curve. Indeed, fault classification is a crucial step for failure diagnosis. The proposed method mainly covers uniform dust faults, partial shading faults, short circuit faults, and aging. The proposed algorithm relies on electrical indicators that are extracted from single diode model and measured I-V curves and used as assessment parameters, the shape assessment parameter is recognized by training a neural network. This method is assessed through a simulation and validated using experimental I-V curves measurements in faulty cases.

Keywords: experimental photovoltaic characterization; I-V curve analysis; photovoltaic model; fault detection algorithm; artificial neural network.

INTRODUCTION

Photovoltaic energy, similarly to other renewable sources, is the best alternative for fulfilling the energy demands, ensuring sustainability and reducing climate changes. Its growth requires advanced methodologies of monitoring systems (1). However, during years of operation of a photovoltaic system, its exposure to the ambient conditions may cause system malfunctions (2). The repetitive occurred faults may reduce the time-life of the module and hasten its aging process, which reduce its efficiency (3).

Fault diagnosis is a fundamental step for reliability, safety and efficiency of photovoltaic monitoring systems (4). Without proper fault detection, non-cleared faults in PV arrays not only cause power losses (5), but also might lead to safety issues. Indeed, implementing reliable and automatic fault detection and diagnostics (FDD) tools will not only mitigate safety concerns but also reduce the operations and maintenance costs associated with PV systems.

Generally, monitoring applications are exploited for fault detection through a drop observation in the energy yield produced by the installation. Thereafter, localization and identification of the fault remain manually handled. Hence, the operator performs an investigation in the faulty PV string in order to locate the malfunctioning module, usually using I-V curve tracer (6). Yet this process may cause time consumption before system recovery. The I-V curve tracing reveals more about the performances of a PV module or array than any measurement method (6). It is also the fastest way to test the performances of a commercial PV array. The I-V curve tracing provides a graphical representation of the array operating characteristics, regarding the changing of the ambient conditions and array problems; it can be exploited as a fault diagnosis tool for solar panel in outdoor operation (7,8).

Methods deployed for fault detection and diagnostic has been a matter of investigation for many years, constituting a great concern in physical system performances in several field (9). FDD methods are often chosen for

Technologies and Materials for Renewable Energy, Environment and Sustainability
AIP Conf. Proc. 2123, 020037-1–020037-14; https://doi.org/10.1063/1.5116964
Published by AIP Publishing. 978-0-7354-1863-9/$30.00

their interest or availability. This approach may have satisfactory results for small scale and laboratory applications but leads to problems in full scale implementations. Which makes proper selection of the most suited detection and diagnosis methods important for a convenient implementation of a reliable FDD tool (10,11).

This paper emphasizes the usefulness of fault detection methodology integration in the photovoltaic monitoring system regarding a convenient approach. At first, faults are classified regarding their nature and influence on the electrical parameter characterizing the PV module. For each fault, we propose an identification method that is mainly based on electrical indicators extracted from characteristics curves. Thus, an online fault detection algorithm is proposed. Experiment measurements are performed for different fault types to validate the algorithm. This latter is upgraded in case of multiple fault occurrences.

For detection methodology, a single diode model regarding operating temperature and irradiation is developed, this tool is used in parallel with real time measurement of the characteristic curve with environmental parameters in outdoor operating condition. Both curves, are used as input for assessment FDD. Afterwards, assessment indicators are extracted from both curves and used in the proposed algorithm.

A neural network is used for shape recognition in case of a deviated curve measurement. The artificial neural network has been trained using several curves measured under different shaded conditions, inducing then many I-V curves with one or more stepped-shape deviation. Its output is a Boolean parameter indicating the existence of the deviation in the tested curve.

PHOTOVOLTAIC FAULT MONITORING

The PV characteristic curve

The I-V curve represents all the possible operating points (current and voltage) of a PV module or string of modules at the existing conditions of sunlight (irradiation) and temperature. The curve starts at the short-circuit current and ends at the open circuit voltage. The maximum power point, located at the knee of the I-V curve, is the operating point that delivers the highest output power, the electrical parameters derived from an I-V curve are the open circuit voltage, the short circuit current, the maximum power point, the fill factor, and the series and shunt resistances. These parameters describe the operation state of the module. Monitoring these values gives a clue about the ambient operating condition regarding irradiation temperature and shadow, and also the inner state of the material, to note the electrical and mechanical mismatches (12). In a healthy PV arrays the value of these parameters should restrain their steady state, any variation in each value refers either to a temporary failure or permanent degradation (13).

An ideal solar cell consists of a single diode connected in parallel with a light generated current source (Ipv). A single diode model including the series resistance R_S considers the voltage drops and internal losses due to flow of current. This model does not adequately represent the behavior of the cell when subjected to environmental variations, especially at low voltage (14). However, a single diode model including the series and parallel resistance is more practical. It considers the leakage current to the ground when the diode is in reversed biased. The output current equation using this model $I=I_{PV}-I_D$ can be written as:

$$I = I_{PV} - I_0\left[\exp\left(\frac{V+IR_s}{\alpha V_T}\right)-1\right]-\left(\frac{V+IR_s}{R_{sh}}\right) \quad (1)$$

Where, Rs and Rp are the equivalent series and parallel resistances, respectively.

I_{PV} is the current created due to the sun light, Io is the reverse saturation current V_T (¼NskT/q) is the module's thermal voltage which having Ns cells connected in series, q is the electron charge (1.60217646 10^{19} C), k is the Boltzmann constant (1.3806503 10^{23} J/K), and T is the temperature of the p–n junction in K and a is the diode ideality factor.

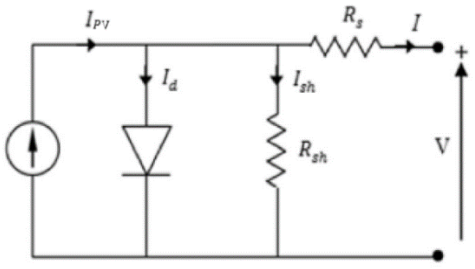

FIGURE 1. Single diode solar cell model

Resolution of the theoretical equation of solar unit requires a numerical methodology.
The light generated current I_{PV} in the nominal condition should be corrected regarding the irradiation and ambient temperature.

$$I_{PV} = \left(I_{pv,n} + K_I \Delta_T\right) \frac{G}{G_n} \tag{2}$$

The diode saturation current has an extreme dependence of the temperature, and it is expressed as following according to [5].

$$I_0 = I_{0,n} \left(\frac{T_n}{T}\right)^3 \exp\left[\frac{qE_g}{\alpha k}\left(\frac{1}{T_n} - \frac{1}{T}\right)\right] \tag{3}$$

Where E_G is band gap energy for the semiconductor, its value is given by 1.12 for polycrystalline, and I_{ON} is the nominal saturation current, it is improved in [5] using temperature dependence with the following formula.

$$I_{0,n} = \frac{I_{sc,n}}{\exp\left(V_{oc,n} \big/ \alpha V_{t,n}\right) - 1} \tag{4}$$

$$I_0 = \frac{I_{sc,n} + K_I \Delta_T}{\exp\left(V_{oc,n} + K_V \Delta_T \big/ \alpha V_t\right) - 1} \tag{5}$$

In the precedent equations, two parameters remain unknown for resolution; that are the shunt and series resistances. Mathematical formulas are found in the literature (15), though it is inevitable that the accurate value of these resistances relies mostly on experimental data. Some authors propose incrementing Rs in an iterative process, until the I-V curve visually fits the experimental data and then vary Rp in the same way. Other authors propose adjusting them as an only pair that warranty the resulting power (16). The overall shape of the characteristic curve is given by numerical equation resolution.

Type of faults through deviation interpretation

Generally, PV system faults can be classified into two types (17): irreversible error caused by mechanical or electrical problems, such as open circuit, short circuits, and PV cell aging; temporary power loss faults that are caused by sheltering, such as cloud shadows. Brief descriptions of those faults in a PV system are found in the literature (18).

The testing of solar modules is required for quality assurance. Deviations of the I-V curve characteristics permits to draw a conclusion concerning the operation condition of the tested module including internal interruption, partial shading, mismatching, and scratches on the frame and excessive or uneven glue marks (5).

The different faulty modes affect the I-V characteristics of the PV module in different ways, leaving distinct signatures during its operation. Fig.2 indicated how the different deviations on the curve could be read.

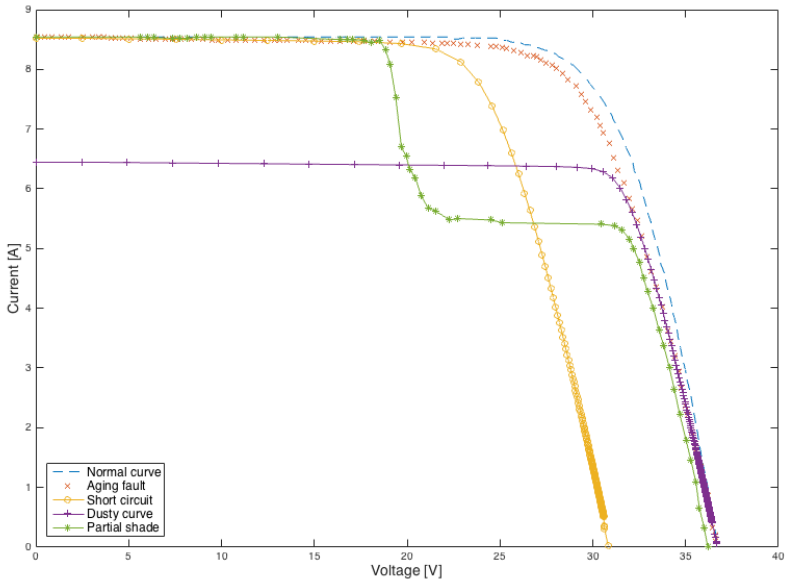

FIGURE 2. I-V curve deviation under different faults.

It should be noted that degradation faults are not treated in this paper; the diagnosis of these types require a deeper study and analysis due to the unexpected and random effect that it has on the electrical output. For instance, sever snail track failure (12) occurrence at cell level leads to bypass diode activation, this type of fault has the same effect as partial shadowing case; which may create a certain confusion if the diagnosis method is not robust enough to differentiate between these two cases.

PROPOSED FAULT IDENTIFICATION METHODOLOGY

The fault detection methodology used is model-based; basically, a model for the photovoltaic module under test is developed and calibrated with its current electrical parameters. The model is under Matlab-Simulink and it simulates the behavior of a reference I-V curve regarding the values of irradiation and ambient temperature. Therefore, a comparing algorithm is performed to specify the nature of the fault occurred. In this study, the effect of each fault on the overall shape of the I-V curve is investigated and observed via outdoor measurements.

Partial shadow

The partial shadowing induces inflexion points on the I-V curve as illustrated in fig.2, the number of these points depends on the shading localization (19). This type of fault is visualized better on the curve, it, of course, reduces the fill factor.

Uniform dust

The uniform dust generally blocks irradiation from reaching the solar cell, which causes a uniform diminishing in the current (20) without inflection points on the I-V curve. It is evaluated through a comparison between the expected short circuit current (corresponding to the measured irradiation) and the measured short-circuit current. The parameter detecting uniform dust is PI.

$$PI = \frac{Isc}{I'sc} * 100 \quad (6)$$

Where I'sc and Isc are, respectively, the simulated short-circuit current and the measured short-circuit current. If the difference is considerable than a cleaning process should be scheduled.

short circuit

The short-circuit fault causes a noticeable drop in the voltage, the current though remains the same as shown in fig.2; it is evaluated with the parameter PV through a comparison between the expected open circuit voltage and the measured open-circuit voltage.

$$PV = \frac{Voc}{V'oc} * 100 \quad (7)$$

Where V'oc and Voc are, respectively, the simulated open circuit voltage and the measured open circuit voltage, the parameter detecting the number of cells short-circuited in α module is given below, where Uoc is the average open circuit voltage of the cells in PV module. In the case where α>10 (21), then a short-circuit fault occurred.

$$\alpha = \frac{(\mathrm{Voc} - \mathrm{V'oc})}{\mathrm{Uoc}} \tag{8}$$

Aging stress/fatigue

The aging faults are more complex to define and recognize. They can influence on a several parameters (Rs, FF, P, I), and cause serious malfunctions in the system. However, in our case, we are dealing with a module in a normal operational mode, where it can be manifested in a certain fatigue in the efficiency of the module by a drop in the value of the fill factor without variation on other parameters (22) as illustrated in fig.2. It is revealed on the I-V curve by a descent on the knee of the curve that can be assessed using the parameter PF.

$$\mathrm{PF} = \frac{\mathrm{Pmp}}{\mathrm{P'mp}} * 100 \tag{9}$$

Where P'mp and Pmp are, respectively, the simulated maximum power and the measured maximum power.

Deviation recognition: Artificial neural network classifier

Artificial Neural Networks (ANN) are adaptive systems, having in entry input variables that are weighted with appropriate internal parameters (weights and bias), being processed through an activation function in order to generate a significant output value (23).

Artificial neural networks are used in a variety of application, permitting the development of adaptive algorithm to all kind of new situations and scenarios (24) through a training process that is performed using a considerable database. Although they have proved their results accuracies, they require few parameters for an optimized training (25). The ANN is used as well in monitoring applications (26) and damage (27) and abnormal behavior (28) detection. Sometimes it can be exploited for activity prediction as in (29). Performing ANN are achieved with either recurrent or dynamic neural networks.

The network learns until obtaining an accurate model of the studied phenomenon. During Back propagation training, matrices of weights and bias are generated, with optimal values in each iteration.

ANNs consider classification as one of the most dynamic research and application areas (23). The ANN classifier has shown great accuracy in fault diagnosis as in (30). Generally, multi-layer feed-forward networks trained using Back Propagation (BP) algorithm seem to be the most significant and widely used method in fault detection and diagnosis systems (26,31). In this work, the final target is to make the ANN able to detect if the input values of current and voltage constitute a curve with one or more inflexion points or not. This is verified through training the network several times with list of data containing inflexion points (that are assigned to the stepped-shape curve) and others measured in faultless conditions (that are assigned to saint curves).

The architecture of the used multi-layer feed-forward neural network is composed of the input layer that is considering the new measured list of current swiping from the short circuit current to the open circuit current (null), hidden layers and the output binary layer that tell if the curve is stepped or not as in fig. 2.

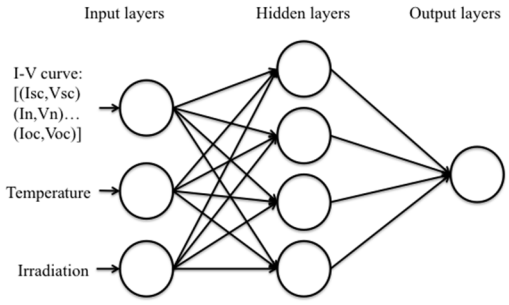

FIGURE 3. Artificial neural network architecture.

Algorithm

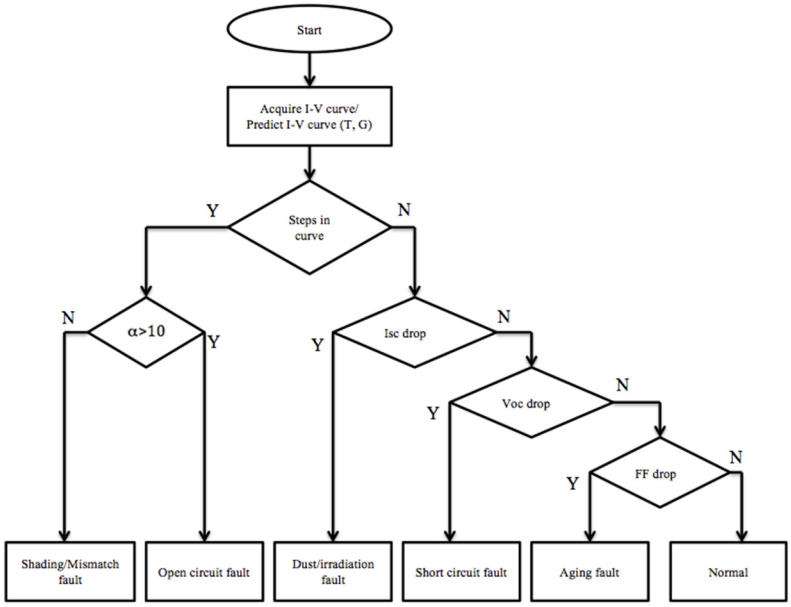

FIGURE 4. Flow chart of fault diagnosis**.**

SIMULATION AND EXPERIMENT VALIDATION

The reference I-V curve is simulated based on a model developed for a crystalline module with the specification indicated in the table below, regarding ambient conditions.

TABLE I. Module specification

Technology	Manufacturer	ISC	VCO	Power
crystalline	Solar World	9.58 (A)	39.4 (V)	275 (W)

The simulation of the curve tracer is performed in Matlab Simulink based on a varying resistive load applied to the theoretical model of the solar panel based on a single diode model (16,32) including series and parallel resistance of a solar panel. These parameters are calibrated with the module under test.

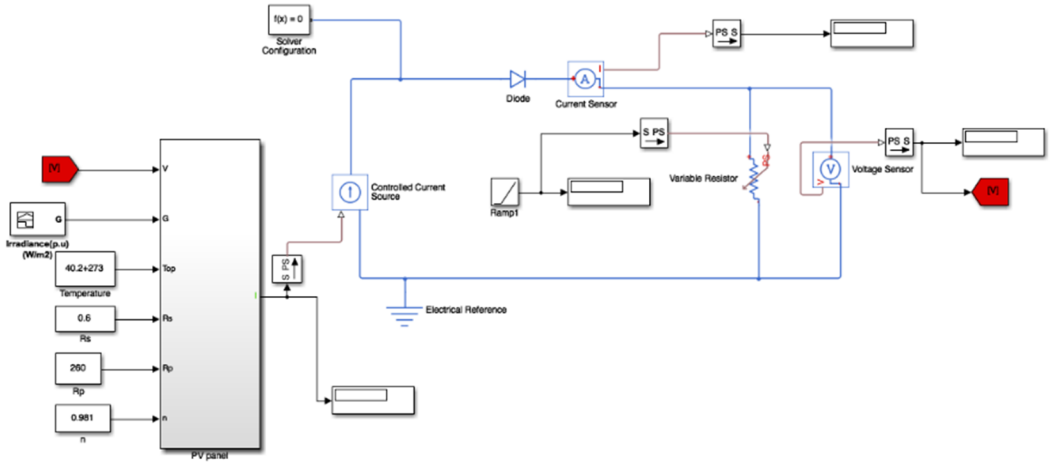

FIGURE 5. Matlab characteristic curve simulation.

FIGURE 6. Experimental Set up: Clean, dusty and shaded solar panels used.

Both curves (Reference and measured) are graphically presented and compared in each faulty case.

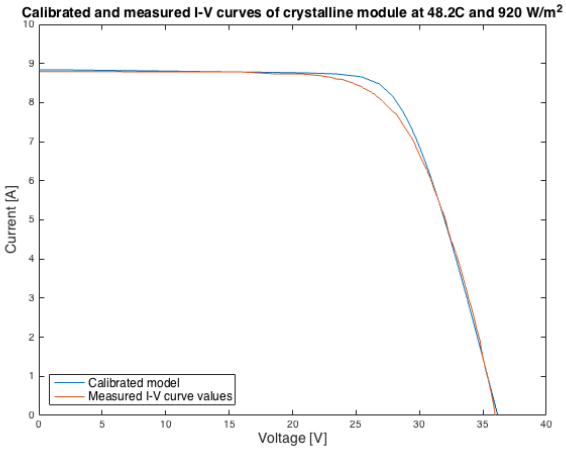

(a)

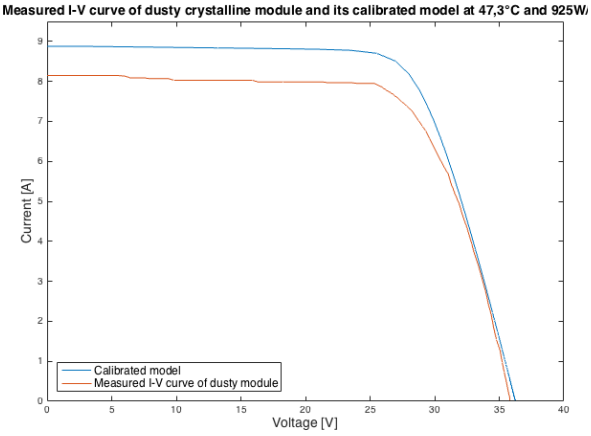

(b)

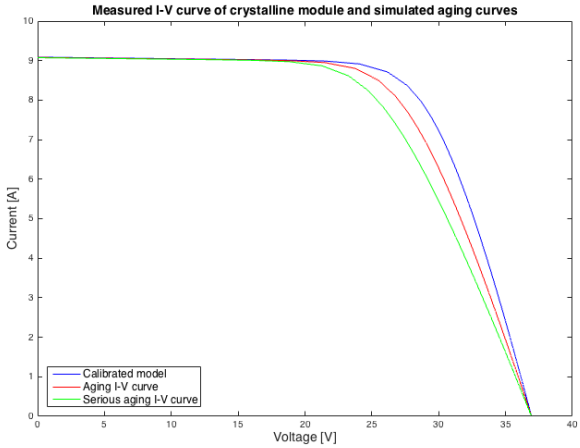

(c)

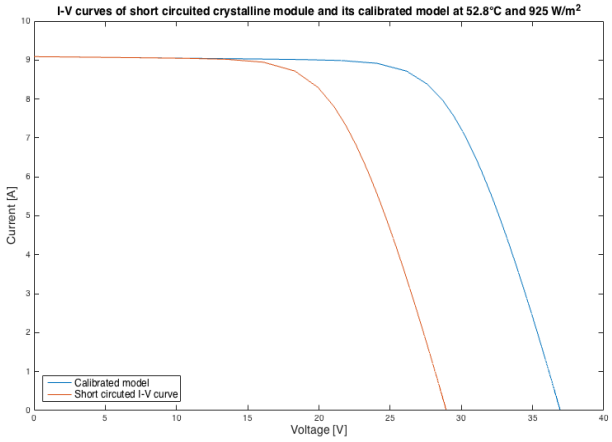

(d)

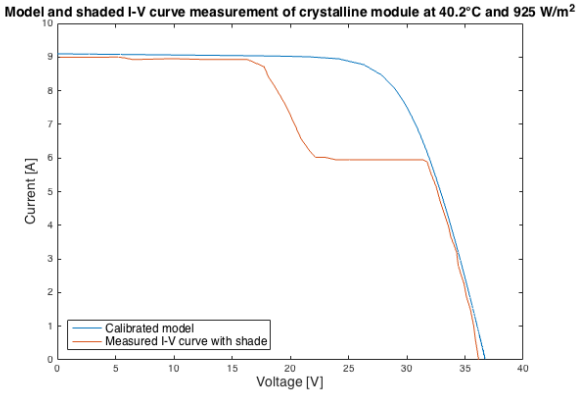

(e)

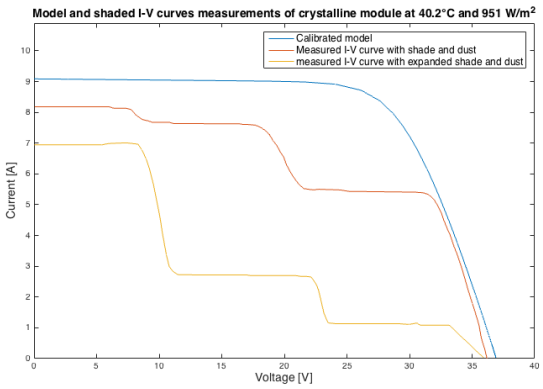

(f)

FIGURE 7. I-V curve measurement under (a) no fault in comparison, (b) uniform dust fault, (c) aging fault, (d) short circuit fault, (e) partial shading fault, (f) both shading and dust faults, with reference curve.

Artificial Neural Network training results

The proposed ANN is trained according to experimental database (measured curve in partial shaded condition) until converging to the target. 70% of the data is used for learning and 15% for testing and 15% for validation. The network is retrained until obtaining a minimal error. Table II shows results after training.

We chose the Levenverg-Marquardt algorithm since it requires less time. This algorithm usually requires more memory but less time. The learning stops automatically when the generalization stops improving, as indicated by the increase in the mean squared error (MSE: MEAN SQUARED ERROR) of the validation samples. The data of the learning are values without defects, in the case where the panel works perfectly. We initiate the learning of our system so that it determines the optimal weights by minimization of error between the exit of the neuron network and the desired exit from the algorithm of retro-propagation of error.

TABLE II. Artificial Neural Network training results

	Samples	**Cross Entropy**	**Error Percentage**
Training	70%	5.12074E-1	16.12903
Testing	15%	9.67982 E-1	14.28571
Validation	15%	9.92205 E-1	14.28571

In order to summarize the performance of the classification algorithm, the confusion matrix technique is set in all training, testing and validation stages. The confusion matrix displays the total number of observations in each cell. The rows of the confusion matrix correspond to the true class, and the columns correspond to the predicted class. Diagonal and off-diagonal cells correspond to correctly and incorrectly classified observations, respectively.

FIGURE 8. Training, validation and test confusion matrixes .

To validate the performance of the network, we have taken the regression graph. The regression graph displays the network outputs against the targets for the learning, validation, and test set. For a perfect fit, the data must fall on a 45-degree line, where the outputs of the network are equal to the targets. For our network, the fit is reasonably good for all data sets, with R values in each case of 0.99. According to the graph of the regression, the margin of error between the target and the output is ±0,00069

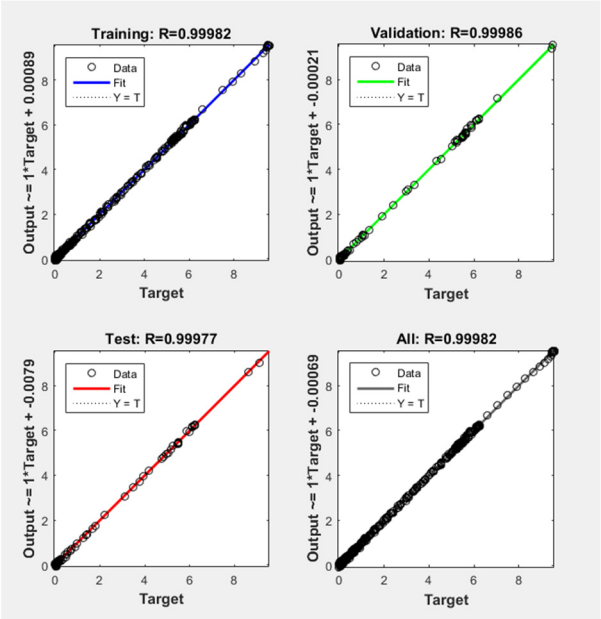

FIGURE 9. The regression graph displaying the network outputs against the targets for the learning.

IMPLEMENTING FAULT DIAGNOSIS SOLUTION

The precedent experiments were exploited in order to elaborate a complete solution for fault detection and diagnosis of a photovoltaic system. The proposed architecture is based on:

- A photovoltaic panel I-V curve measurement tool, operating in the outdoor; taking the real operating measurements of the module under test, measuring the temperature and the irradiation as well.
- An I-V curve simulator based on a varying resistor implemented with a single diode model taking as input the characteristics of the module under test with the measured temperature and irradiation.
- The developed algorithm for FDD.

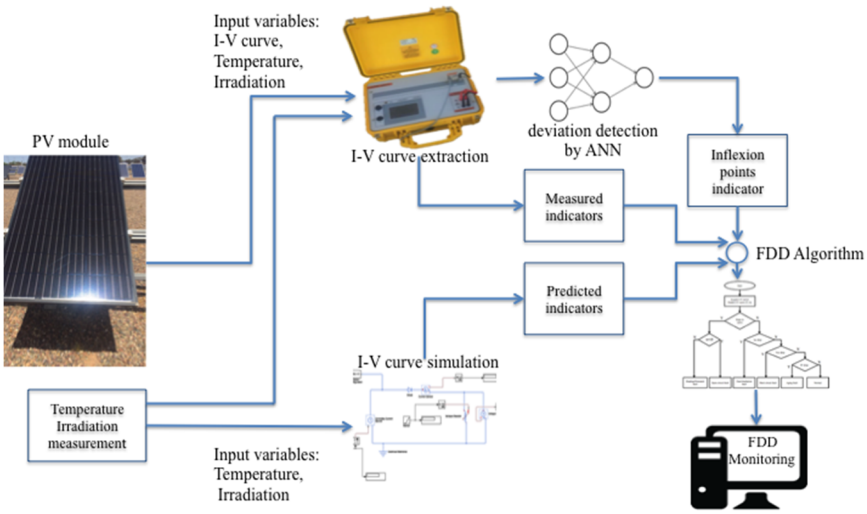

FIGURE 10. Fault detection and diagnosis solution architecture.

The diagram below describes the training of the network. It shows that after the 28 iterations, the desired result is reached. With 5 hidden neurons, the three curves relating to the evolution of the mean squared error of the three phases (Training, Validation, Test) converge correctly towards the minimum of squared mean error (MSE = 0.0022282). The network was trained until reaching the phase of over-learning, this phenomenon was met after 34 iterations. It is interesting to continue learning until you reach this phase for the test in order to perfect the network. So, the result is reasonable all the while with the following considerations:

- The mean squared error is small.
- The test error and the validation error have similar characteristics.
- There is no significant over-learning by iteration 28 (where the best validation performance takes place).

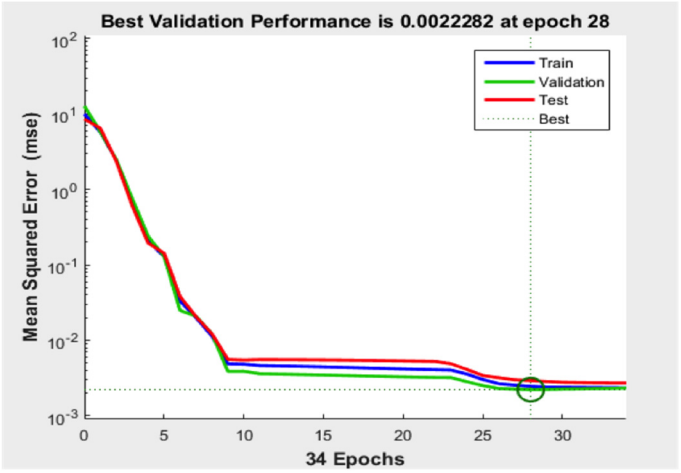

FIGURE 11. Performance diagram of the diagnosis solution.

RESULTS VALIDATION AND DISCUSSION

After experimental measurement of different classified faults, it is observed that each fault has a different signature on the shape of the I-V curve. To determine the nature of the fault the calculated parameters compare each measured value with its reference value. Then, the algorithm implemented used these parameters to diagnosis the occurred faults.

TABLE III. Simulated and measured values comparison

Cases	Simulated Short Circuit Current	Measured Short Circuit Current	Simulated Open Circuit Voltage	Measured Open Circuit Voltage	Step
a	8.83	8.79	36.14	36	No
e	9.08	8.98	36.87	36.19	Yes
b	8.88	8.14	36.15	35.81	No
d	9.09	9.09	36.95	28.98	No
c-red	9.14	9.14	36.93	36.93	No
c-green	9.14	9.14	36.93	36.93	No
f-yellow	9.09	6.94	36.9	35.9	Yes

In this study, the developed PV model simulates for each case, the I-V curve and extracts the parameters, which are short circuit current, open circuit voltage and fill factor depending on the measured temperature and irradiation. The evaluation of these parameters within the measured ones permits drawing a conclusion about system's status as mentioned earlier. Also, steps in the measured curve are considered.

By comparing the simulated current, voltage and FF with the measured ones of each measurement point, abnormal losses are observed in case F. However, the measured curve in case A is closed to the predicted curve model. In cases B and F steps are spotted in the measured curve, whereas in cases C and D considerable voltage or current drop.

In the following table, each of assessment parameters used in the algorithm is calculated for all measured cases.

TABLE IV. calculated values for delecting faults

Cases	Steps	Alpha	PI	PV	PF
a	-	0.233	99.546	99.612	95.558
e	Yes	1.133	98.898	98.155	83.213
b	-	0.566	91.666	99.059	90.505
d	-	13.288	100	78.430	72.171
c-red	-	0	100	100	94.094
c-green	-	0	100	100	88.258
f-yellow	Yes	1.666	76.347	97.289	25.344

Finally, through precedent parameters evaluation, the following table sums up the results obtained in each case. It's worth mentioning that the developed algorithm permits several faults diagnosis as in case F.

TABLE V. Assessment table for each case

Cases	Shade	Dust	Short circuit	Aging	Normal
a	-	-	-	-	Yes
e	Yes	-	-	-	-
b	-	Yes	-	-	-
d	-	-	Yes	-	-
c-red	-	-	-	Little aging	-
c-green	-	-	-	Serious aging	-
f -yellow	Yes	Yes	-	-	-

Results interpretation

From this work we conclude:

Based on the comparison of the simulated curve with the measured curve of PV module, a deviation interpretation permits making conclusions about fault the may occur in the system, basically, shading, mismatches and disconnected cells are responsible for visualization for steps in the I-V curve.

- For shape assessment of a measured I-V curve, a trained neural network can determine weather deviation or step is in a series of measured points or not.
- When a module is uniformly dusty the measured short circuit current is lower than the simulated short circuit current in the same ambient conditions.
- It can determine whether open-circuit has occurred by comparing the measured open circuit voltage and the simulated open circuit voltage.
- When a module is short-circuited fault, the number of short-circuited cells can be calculated based on the open circuit voltage.
- The value of fill factor will decrease when aging fault occurs. If it is less than 0.7, it can be judged that the aging fault has occurred.

Method application

The above algorithm permits detecting faults in the photovoltaic system in many cases as presented in table IV. The results of this algorithm are used as an input to the generated alarm in the monitoring system for the end of fast intervention. Hence, the duration of operations and maintenance (O&M) are reduced.

The method limitation resides in the learning algorithm that needs a huge amount of data for training the network in order to be reliable to detect all sort of deviation in any measured curve. Another limitation of the integral solution is the occurrence of failure (12,33) that might have similar signature on the measured I-V curve that might generate confusion at the output of the proposed algorithm.

CONCLUSION

Fault monitoring is indispensable for ensuring that photovoltaic systems run in a safe and reliable status. Automatic fault detection and classification remains a major challenge in the PV monitoring filed. In this paper, a diagnosis methodology based on characteristics curve deviation analysis was presented. The detection of the faulty cases was based on experimental measurement compared to a developed model of the PV system. The identification of the fault's nature was performed through the presented algorithm, which assesses the electrical parameters and tests the inflexion points in a measured curve base on a learning algorithm.

The purpose of this paper was the automation of system detection, based on fault recognition extracted from the measured characteristic. This aims to facilitate decision making for O&M sake. Gaining in terms of algorithm efficiency and reliability require upgrading the proposed methodology and correlating it with other diagnosis methodologies that are used in the industry.

ACKNOWLEDGMENT

This work is supported by IRESEN (Research Institute in Solar Energy and Renewable Energies), GREEN ENERGY PARK RESEARCH PLATFORM BENGUERIR, MOROCCO.

The authors would like to acknowledge the contribution of Mrs. Boubou bouchra.

REFERENCES

1. Madeti SR, Singh SN. Monitoring system for photovoltaic plants: A review. Renewable and Sustainable Energy Reviews. 2017 Jan;67:1180–207.
2. Kumar M, Kumar A. Performance assessment and degradation analysis of solar photovoltaic technologies: A review. Renewable and Sustainable Energy Reviews. 2017 Oct;78:554–87.
3. Ndiaye A, Charki A, Kobi A, Kébé CMF, Ndiaye PA, Sambou V. Degradations of silicon photovoltaic modules: A literature review. Solar Energy. 2013 Oct;96:140–51.
4. Harrou F, Sun Y, Taghezouit B, Saidi A, Hamlati M-E. Reliable fault detection and diagnosis of photovoltaic systems based on statistical monitoring approaches. Renewable Energy. 2018 Feb;116:22–37.

5. Köntges M, Kurtz S, Packard C, Jahn U, Berger KA, Kato K. Performance and reliability of photovoltaic systems: subtask 3.2: Review of failures of photovoltaic modules: IEA PVPS task 13: external final report IEA-PVPS. Sankt Ursen: International Energy Agency, Photovoltaic Power Systems Programme; 2014. 132 p.
6. Zhao Y. Fault detection, classification and protection in solar photovoltaic arrays. [Boston, Massachusetts]: Northeastern University, Boston, Massachusetts; 2015.
7. Quiroz JE, Stein JS, Carmignani CK, Gillispie K. In-situ module-level I–V tracers for novel PV monitoring. In IEEE; 2015 [cited 2018 Apr 26]. p. 1–6. Available from: http://ieeexplore.ieee.org/document/7355608/
8. Wang W, Liu AC-F, Chung HS-H, Lau RW-H, Zhang J, Lo AW-L. Fault Diagnosis of Photovoltaic Panels Using Dynamic Current–Voltage Characteristics. IEEE Transactions on Power Electronics. 2016 Feb;31(2):1588–99.
9. Katipamula S, Brambley M. Review Article: Methods for Fault Detection, Diagnostics, and Prognostics for Building Systems—A Review, Part I. HVAC&R Research. 2005 Jan 1;11(1):3–25.
10. Triki-Lahiani A, Bennani-Ben Abdelghani A, Slama-Belkhodja I. Fault detection and monitoring systems for photovoltaic installations: A review. Renewable and Sustainable Energy Reviews. 2018 Feb;82:2680–92.
11. Chao K-H, Chen C-T. A remote supervision fault diagnosis meter for photovoltaic power generation systems. Measurement. 2017 Jul;104:93–104.
12. Tsanakas JA, Ha L, Buerhop C. Faults and infrared thermographic diagnosis in operating c-Si photovoltaic modules: A review of research and future challenges. Renewable and Sustainable Energy Reviews. 2016 Sep;62:695–709.
13. Hernday P. Guide To Interpreting I-V Curve Measurements of PV Arrays [Internet]. Solmetric; 2011 [cited 2018 Apr 26]. Available from: http://resources.solmetric.com/get/Guide%20to%20Interpreting%20I-V%20Curves.pdf
14. Ishaque K, Salam Z, Taheri H. Simple, fast and accurate two-diode model for photovoltaic modules. Solar Energy Materials and Solar Cells. 2011 Feb;95(2):586–94.
15. Chenni R, Makhlouf M, Kerbache T, Bouzid A. A detailed modeling method for photovoltaic cells. Energy. 2007 Sep;32(9):1724–30.
16. Villalva MG, Gazoli JR, Filho ER. Comprehensive Approach to Modeling and Simulation of Photovoltaic Arrays. IEEE Transactions on Power Electronics. 2009 May;24(5):1198–208.
17. Ji D, Zhang C, Lv M, Ma Y, Guan N. Photovoltaic Array Fault Detection by Automatic Reconfiguration. Energies. 2017 May 16;10(5):699.
18. Sarikh S, Raoufi M, Bennouna A, Benlarabi A, Ikken B. Fault diagnosis in a photovoltaic system through I-V characteristics analysis. In: 2018 9th International Renewable Energy Congress (IREC) [Internet]. Hammamet: IEEE; 2018 [cited 2018 Dec 16]. p. 1–6. Available from: https://ieeexplore.ieee.org/document/8362572/
19. Salem F, Awadallah MA. Detection and assessment of partial shading in photovoltaic arrays. Journal of Electrical Systems and Information Technology. 2016 May;3(1):23–32.
20. Rao A, Pillai R, Mani M, Ramamurthy P. Influence of Dust Deposition on Photovoltaic Panel Performance. Energy Procedia. 2014;54:690–700.
21. Chen YH, Liang R, Tian Y, Wang F. A novel fault diagnosis method of PV based-on power loss and I-V characteristics. IOP Conference Series: Earth and Environmental Science. 2016 Aug;40:012022.
22. Chunlai L, Xianshuang Z, Gudake. A Survey of Online Fault Diagnosis for PV Module Based on BP Neural Network. In IEEE; 2016 [cited 2018 Apr 26]. p. 483–6. Available from: http://ieeexplore.ieee.org/document/7825145/
23. K S, S S. Review on Classification Based on Artificial Neural Networks. The International Journal of Ambient Systems and Applications. 2014 Dec 31;2(4):11–8.
24. Paliwal M, Kumar UA. Neural networks and statistical techniques: A review of applications. Expert Systems with Applications. 2009 Jan;36(1):2–17.
25. Markou M, Singh S. Novelty detection: a review—part 2: Signal Processing. 2003 Dec;83(12):2499–521.
26. Rafiee J, Arvani F, Harifi A, Sadeghi MH. Intelligent condition monitoring of a gearbox using artificial neural network. Mechanical Systems and Signal Processing. 2007 May;21(4):1746–54.
27. Bakhary N, Hao H, Deeks AJ. Damage detection using artificial neural network with consideration of uncertainties. Engineering Structures. 2007 Nov;29(11):2806–15.
28. Arifoglu D, Bouchachia A. Activity Recognition and Abnormal Behaviour Detection with Recurrent Neural Networks. Procedia Computer Science. 2017;110:86–93.

29. Jacobé de Naurois C, Bourdin C, Stratulat A, Diaz E, Vercher J-L. Detection and prediction of driver drowsiness using artificial neural network models. Accident Analysis & Prevention [Internet]. 2017 Dec [cited 2018 Apr 26]; Available from: http://linkinghub.elsevier.com/retrieve/pii/S0001457517304347
30. Pohjoranta A, Sorrentino M, Pianese C, Amatruda F, Hottinen T. Validation of Neural Network-based Fault Diagnosis for Multi-stack Fuel Cell Systems: Stack Voltage Deviation Detection. Energy Procedia. 2015 Dec;81:173–81.
31. Chen Z, Wu L, Cheng S, Lin P, Wu Y, Lin W. Intelligent fault diagnosis of photovoltaic arrays based on optimized kernel extreme learning machine and I-V characteristics. Applied Energy. 2017 Oct;204:912–31.
32. Sarikh S, Raoufi M, Benlarabi A, Ikken B. PV Performance Assessment Through Calibrated Modeling And Experimental Characterization. In Tangier, Morocco: IEEE; 2018. p. 6. Available from: https://ieeexplore.ieee.org/document/8477277
33. Sarikh S, Raoufi M, Bennouna A, Benlarabi A, Ikken B. Photovoltaic Discoloration and Cracks: Experimental Impact on the I-V Curve Degradation. In: Hajji B, Tina GM, Ghoumid K, Rabhi A, Mellit A, editors. Proceedings of the 1st International Conference on Electronic Engineering and Renewable Energy [Internet]. Singapore: Springer Singapore; 2019 [cited 2018 Dec 17]. p. 609–16. Available from: http://link.springer.com/10.1007/978-981-13-1405-6_69